ELASTIC-VISCOPLASTIC ANALYSIS OF ULTRA-FINE PLATE-FIN STRUCTURES WITH LAMINATE MISALIGNMENT USING A HOMOGENIZATION THEORY

N. Yamamoto[1], T. Matsuda[1]*
[1] Department of Engineering Mechanics and Energy, University of Tsukuba, Tsukuba, Japan
* Corresponding author (matsuda@kz.tsukuba.ac.jp)

Keywords: *Plate-fin structure, Laminate Misalignment, Homogenization, Viscoplasticity, Compressibility*

1 Introduction

Ultra-fine plate-fin structures for heat exchangers, manufactured by stacking thin metallic plates and fins alternately (Fig. 1) offer high heat exchanger efficiency, because their small structures provide large heat-transfer areas. Thus, they are expected to be used in the heat exchangers of high temperature gas-cooled reactor gas-turbine (HTGR-GT) systems [1,2]. The HTGR-GT systems are regarded as some of the most promising power generating systems because of their excellent balance between power generation and economic efficiency [3]. In the systems, helium is employed as a working fluid, which becomes extremely hot and can reach 950 °C. It is therefore important to analyze not only elastic behavior but also inelastic behavior of ultra-fine plate-fin structures.

In general, fins in an ultra-fine plate-fin structure are not necessarily stacked in such a precisely-aligned position as illustrated in Fig. 1(a), but can have misalignment randomly as shown in Fig. 1(b). Thus, when analyzing the elastic/inelastic behavior of ultra-fine plate-fin structures, such laminate misalignment should be taken into account. So far, however, the effects of laminate misalignment on the elastic/inelastic behavior of plate-fin structures have not been discussed, although there have been some reports on elastic/inelastic analysis of plate-fin structures [1,2,4]. For example, Kawashima et al. [2] performed the elastic-plastic analysis of ultra-fine plate-fin structures based on the finite element method (FEM). In the analysis, however, by referring to their test specimens, they adopted an FE model which had only three layers and two columns of fins without laminate misalignment. More recently, Tsuda et al. [4] analyzed the macroscopic elastic-viscoplastic behavior of ultra-fine plate-fin structures based on a homogenization technique using the FEM, and succeeded in developing a macroscopic constitutive model which can reproduce the homogenized elastic-viscoplastic behavior of plate-fin structures. In their study, however, they used a unit cell approach with the periodic boundary condition, resulting in no consideration for laminate misalignment.

In this study, the elastic-viscoplastic analysis of ultra-fine plate-fin structures with random laminate

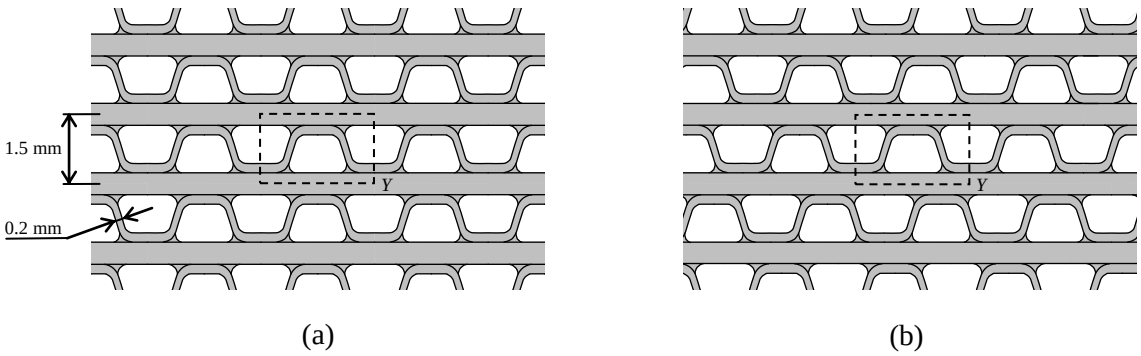

Fig. 1. Ultra-fine plate-fin structures (a) without laminate misalignment, (b) with random laminate misalignment.

misalignment is performed using the time-dependent homogenization theory [5] in conjunction with the substructure method [6]. For this, a unit cell of a plate-fin structure with randomly misaligned N layers of fins is defined. The Y-periodic boundary condition is used on the side boundary surfaces of the unit cell. On the other hand, the boundary condition for periodic laminate misalignment proposed by the authors [7, 8] is applied on the top and bottom boundary surfaces. The unit cell is then divided into N substructures to introduce the substructure method into the time-dependet homogenization theory. Using the present method, elastic-viscoplastic behavior of ultra-fine plate-fin structures with randomly misaligned 10-100 layers is analyzed to investigate the effects of laminate misalignment on the elastic-viscoplastic properties of plate-fin structures.

2 Homogenization Theory for Plate-Fin Structures with Random Laminate Misalignment

2.1 Ultra-Fine Plate-Fin Structure with Random Laminate Misalignment and Its Unit Cell

We consider an ultra-fine plate-fin structure with random laminate misalignment illustrated in Fig. 2, in which, exactly, a plate-fin structure with randomly laminated N fin layers is repeated in the y_2-direction with periodic misalignment. The plate-fin structure has the same shape infinitely in the y_3-direction.

For the ultra-fine plate-fin structure with random laminate misalignment, a unit cell Y and the Cartesian coordinates y_i $(i = 1, 2, 3)$ are defined as shown in Fig. 2(a). The original Y-periodic boundary condition is used on the side boundary surfaces of Y, while the boundary condition for periodic laminate misalignment [7, 8] is applied to the upper and bottom boundary surfaces, which will be fully described in the following subsection.

2.2 Time-Dependent Homogenization Theory

Microscopic stress and strain fields are denoted by σ_{ij} and ε_{ij}, respectively. Then, the equilibrium of σ_{ij} can be expressed in a rate form as

$$\dot{\sigma}_{ij,j} = 0, \tag{1}$$

where $(\dot{\ })$ and $(\ )_{,j}$ indicate the differentiation regarding t and y_j, respectively. The base material of the plate-fin structure is assumed to exhibit linear elasticity and non-linear viscoplasticity as characterized by

$$\dot{\sigma}_{ij} = c_{ijkl}(\dot{\varepsilon}_{kl} - \beta_{kl}), \tag{2}$$

where c_{ijkl} and β_{kl} stand for the elastic stiffness and

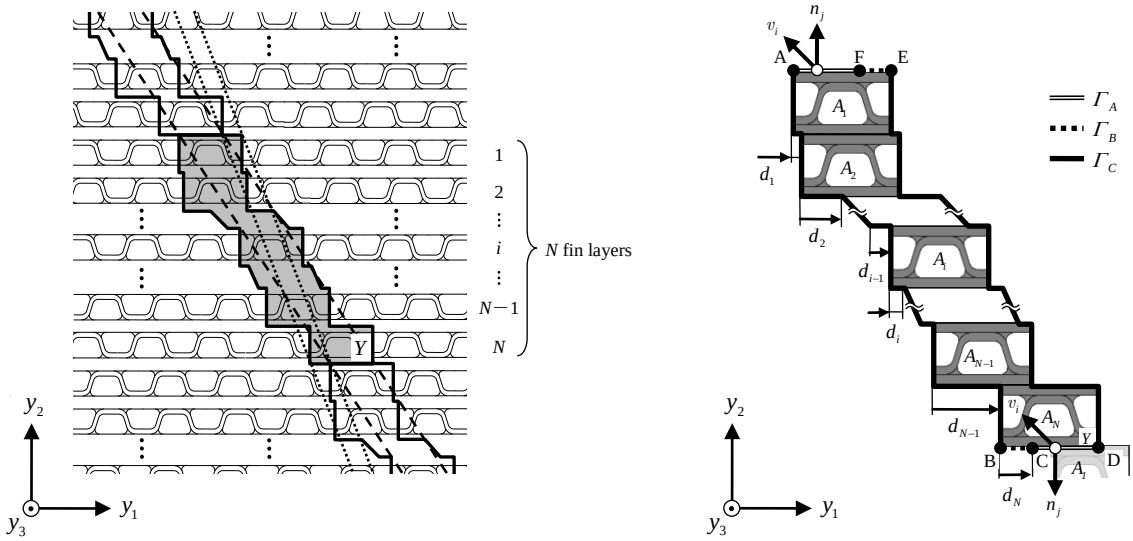

Fig. 2. Ultra-fine plate-fin structure with random laminate misalignment; (a) whole structure and its unit cell Y, (b) unit cell Y and substructures A_i.

viscoplastic strain rate of the base material, respectively.

Let $v_i(\boldsymbol{y},t)$ be an arbitrary variation of the perturbed velocity field defined in Y at t. Then, the integration by parts and the divergence theorem allow Eq. (1) to be transformed to

$$\int_Y \dot{\sigma}_{ij} v_{i,j} dY - \int_\Gamma \dot{\sigma}_{ij} n_j v_i d\Gamma = 0, \tag{3}$$

where Γ denotes the boundary of Y, and n_j indicates the unit vector outward normal to Γ.

Now, consider that Γ is divided into three parts, Γ_A, Γ_B and Γ_C, as shown in Fig. 2(b). This allows the boundary integral term in the above equation to be divided into three terms:

$$\int_\Gamma \dot{\sigma}_{ij} n_j v_i d\Gamma = \int_{\Gamma_A} \dot{\sigma}_{ij} n_j v_i d\Gamma_A + \int_{\Gamma_B} \dot{\sigma}_{ij} n_j v_i d\Gamma_B + \int_{\Gamma_C} \dot{\sigma}_{ij} n_j v_i d\Gamma_C. \tag{4}$$

First, focus on the first term on the right-hand side in the above equation, which is for Γ_A. Figure 2(b) shows that the distributions of $\dot{\sigma}_{ij}$ and v_i on AF and those on CD are identical, respectively, because the internal structure of the plate-fin structure has periodicity in the direction indicated by the dashed lines as shown in Fig 2(a). Whereas, n_j takes opposite directions on AF and CD. As a result, the first term on the right-hand side in Eq. (4) becomes zero. The same situation exists on FE and BC, which belong to Γ_B, as depicted in Fig. 2(b). This allows the second term on the right-hand side in Eq. (4) to be zero. By contrast, on AB and ED, the usual Y-periodicity is satisfied as seen from Fig. 2(a). Hence, the third term on the right-hand side in Eq. (4) also becomes zero. Consequently, Eq. (4) vanishes, and Eq. (3) results in:

$$\int_Y \dot{\sigma}_{ij} v_{i,j} dY = 0. \tag{5}$$

This resulting equation has the same form as that obtained in the previous study [5]. Therefore, the evolution equation of microscopic stress σ_{ij} and the relation between macroscopic stress rate $\dot{\Sigma}_{ij}$ and strain rate $\dot{E}_{kl}$ are derived in the same procedure as the previous study [5]:

$$\dot{\sigma}_{ij} = c_{ijpq}\left(\delta_{pk}\delta_{ql} + \chi^{kl}_{p,q}\right)\dot{E}_{kl} - c_{ijkl}\left(\beta_{kl} - \varphi_{k,l}\right), \tag{6}$$

$$\dot{\Sigma}_{ij} = \left\langle c_{ijpq}\left(\delta_{pk}\delta_{ql} + \chi^{kl}_{p,q}\right)\right\rangle \dot{E}_{kl} - \left\langle c_{ijkl}\left(\beta_{kl} - \varphi_{k,l}\right)\right\rangle, \tag{7}$$

where δ_{ij} indicates Kronecker's delta, and $\langle\ \rangle$ designates the volume average in Y defined as $\langle \# \rangle = |Y|^{-1}\int_Y \# dY$, in which $|Y|$ signifies the volume of Y. Moreover, χ^{kl}_i and φ_i in Eqs. (6) and (7) denote the characteristic functions determined by solving the following boundary value problems:

$$\int_Y c_{ijpq}\chi^{kl}_{p,q} v_{i,j} dY = -\int_Y c_{ijkl} v_{i,j} dY, \tag{8}$$

$$\int_Y c_{ijpq}\varphi_{p,q} v_{i,j} dY = \int_Y c_{ijkl}\beta_{kl} v_{i,j} dY. \tag{9}$$

It should be noted that, when solving the above problems, the periodicity on AF and CD, FE and BC, and AB and ED are imposed on χ^{kl}_i and φ_i.

2.3 Substructure Method

First, the unit cell Y is divided into substructures A_i $(i = 1, 2, \ldots, N)$ as shown in Fig. 2(b). In addition, the amount of laminate misalignment between A_i is defined as d_i $(i = 1, 2, \ldots, N)$. Then, the boundary value problems for the individual substructure in a finite element discretized form are derived as follows [6]:

$$\boldsymbol{k}\boldsymbol{\chi}^{kl}_i = \boldsymbol{f}^{kl}, (i = 1, 2, \ldots, N), \tag{10}$$

$$\boldsymbol{k}\boldsymbol{\varphi}_i = \boldsymbol{g}_i, (i = 1, 2, \ldots, N), \tag{11}$$

where $\boldsymbol{\chi}^{kl}_i$ and $\boldsymbol{\varphi}_i$ denote the nodal vector of characteristic functions in A_i, and $\boldsymbol{k}$, $\boldsymbol{f}^{kl}$ and $\boldsymbol{g}_i$ have the following expressions:

$$\boldsymbol{k} = \int_A \boldsymbol{B}^{\mathrm{T}}\boldsymbol{C}\boldsymbol{B} dA, \tag{12}$$

$$\boldsymbol{f}^{kl} = -\int_A \boldsymbol{B}^{\mathrm{T}}\boldsymbol{C}^{kl} dA, \tag{13}$$

$$\boldsymbol{g}_i = \int_{A_i} \boldsymbol{B}^{\mathrm{T}}\boldsymbol{C}^{kl}\boldsymbol{\beta} dA_i. \tag{14}$$

Next, the components of $\boldsymbol{\chi}^{kl}_i$ and $\boldsymbol{\varphi}_i$ are respectively divided into two parts, $\boldsymbol{\chi}^{kl(\Omega)}_i$ and $\boldsymbol{\chi}^{kl(\Gamma)}_i$, and $\boldsymbol{\varphi}^{(\Omega)}_i$ and $\boldsymbol{\varphi}^{(\Gamma)}_i$, where $(\ )^{(\Omega)}$ and $(\ )^{(\Gamma)}$ represent vectors or matrices for the internal and the boundary nodes of A_i, respectively. Then, the boundary value problems for A_i, Eqs. (10) and (11), are rewritten into the following equations:

$$\begin{bmatrix} \boldsymbol{k}^{(\Omega)} & \boldsymbol{k}^{(\Omega\Gamma)} \\ \boldsymbol{k}^{(\Gamma\Omega)} & \boldsymbol{k}^{(\Gamma)} \end{bmatrix} \begin{Bmatrix} \boldsymbol{\chi}^{kl(\Omega)}_i \\ \boldsymbol{\chi}^{kl(\Gamma)}_i \end{Bmatrix} = \begin{Bmatrix} \boldsymbol{f}^{kl(\Omega)} \\ \boldsymbol{f}^{kl(\Gamma)} \end{Bmatrix}, \tag{15}$$

$$\begin{bmatrix} \boldsymbol{k}^{(\Omega)} & \boldsymbol{k}^{(\Omega\Gamma)} \\ \boldsymbol{k}^{(\Gamma\Omega)} & \boldsymbol{k}^{(\Gamma)} \end{bmatrix} \begin{Bmatrix} \boldsymbol{\varphi}^{(\Omega)}_i \\ \boldsymbol{\varphi}^{(\Gamma)}_i \end{Bmatrix} = \begin{Bmatrix} \boldsymbol{g}^{(\Omega)}_i \\ \boldsymbol{g}^{(\Gamma)}_i \end{Bmatrix}, \tag{16}$$

where $\boldsymbol{\chi}^{kl(\Omega)}_i$ and $\boldsymbol{\varphi}^{(\Omega)}_i$ can be expressed as

$$\boldsymbol{\chi}^{kl(\Omega)}_i = \left(\boldsymbol{k}^{(\Omega)}\right)^{-1}\left(\boldsymbol{f}^{kl(\Omega)} - \boldsymbol{k}^{(\Omega\Gamma)}\boldsymbol{\chi}^{kl(\Gamma)}_i\right), \tag{17}$$

$$\boldsymbol{\varphi}^{(\Omega)}_i = \left(\boldsymbol{k}^{(\Omega)}\right)^{-1}\left(\boldsymbol{g}^{kl(\Omega)}_i - \boldsymbol{k}^{(\Omega\Gamma)}\boldsymbol{g}^{kl(\Gamma)}_i\right). \tag{18}$$

The eliminations of $\boldsymbol{\chi}^{kl(\Omega)}_i$ and $\boldsymbol{\varphi}^{(\Omega)}_i$ from Eqs. (15) and (16) using the above equations respectively yields

$$\bar{\boldsymbol{k}}^{(\Gamma)}\boldsymbol{\chi}_i^{kl(\Gamma)} = \bar{\boldsymbol{f}}^{kl(\Gamma)}, \tag{19}$$

$$\bar{\boldsymbol{k}}^{(\Gamma)}\boldsymbol{\varphi}_i^{(\Gamma)} = \bar{\boldsymbol{g}}_i^{(\Gamma)}, \tag{20}$$

where $\bar{\boldsymbol{k}}^{(\Gamma)}$, $\bar{\boldsymbol{f}}^{kl(\Gamma)}$ and $\bar{\boldsymbol{g}}_i^{(\Gamma)}$ are expressed as follows:

$$\bar{\boldsymbol{k}}^{(\Gamma)} = \boldsymbol{k}^{(\Gamma)} - \boldsymbol{k}^{(\Gamma\Omega)}\left(\boldsymbol{k}^{(\Omega)}\right)^{-1}\boldsymbol{k}^{(\Omega\Gamma)}, \tag{21}$$

$$\bar{\boldsymbol{f}}^{kl(\Gamma)} = \boldsymbol{f}^{kl(\Gamma)} - \boldsymbol{k}^{(\Gamma\Omega)}\left(\boldsymbol{k}^{(\Omega)}\right)^{-1}\boldsymbol{f}^{kl(\Omega)}, \tag{22}$$

$$\bar{\boldsymbol{g}}_i^{(\Gamma)} = \boldsymbol{g}_i^{(\Gamma)} - \boldsymbol{k}^{(\Gamma\Omega)}\left(\boldsymbol{k}^{(\Omega)}\right)^{-1}\boldsymbol{g}_i^{(\Omega)}. \tag{23}$$

Finally, Eqs. (19) and (20) are respectively assembled into the following equations, which are boundary value problems with respect to just the boundary nodes of all substructures:

$$\boldsymbol{K}^{(\Gamma)}\boldsymbol{\chi}^{kl(\Gamma)} = \boldsymbol{F}^{kl(\Gamma)}, \tag{24}$$

$$\boldsymbol{K}^{(\Gamma)}\boldsymbol{\varphi}^{(\Gamma)} = \boldsymbol{G}^{(\Gamma)}, \tag{25}$$

where $\boldsymbol{K}^{(\Gamma)}$ stands for the matrix consisting of $\bar{\boldsymbol{k}}^{(\Gamma)}$, $\boldsymbol{F}^{kl(\Gamma)}$ and $\boldsymbol{G}^{(\Gamma)}$ indicates the vector consisting of $\bar{\boldsymbol{f}}^{kl(\Gamma)}$ and $\bar{\boldsymbol{g}}_i^{(\Gamma)}$. Moreover, $\boldsymbol{\chi}^{kl(\Gamma)}$ and $\boldsymbol{\varphi}^{(\Gamma)}$ denote the nodal vectors of the characteristic functions at the boundary nodes of substructures. The characteristic functions $\boldsymbol{\chi}^{kl(\Gamma)}$ and $\boldsymbol{\varphi}^{(\Gamma)}$ are determined by solving Eq. (24) and (25) with appropriate boundary conditions. Then, the characteristic functions at the internal nodes, $\boldsymbol{\chi}_i^{kl(\Omega)}$ and $\boldsymbol{\varphi}_i^{(\Omega)}$, are calculated using Eqs. (17) and (18).

3 Analysis Conditions

In the present analysis, macroscopic stress-strain relations and macroscopic compressibility of ultra-fine plate-fin structures with random laminate misalignment at 900°C were analyzed using the above-mentioned theory.

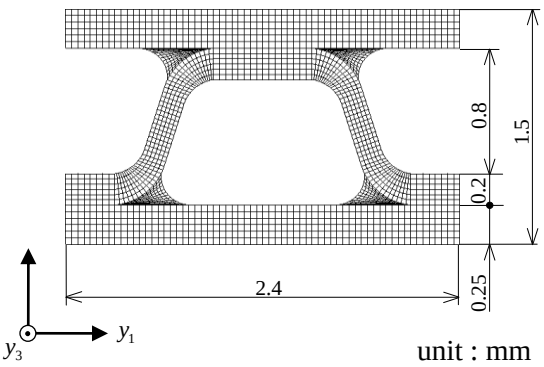

Fig. 3. Substructures A_i and finite element mesh.

Table 1. Material constants of Hastelloy X at 900°C [4].

Young's modulus	E [GPa]	131.4
Poisson's ratio	ν	0.30
Reference strain rate	$\dot{\varepsilon}_0$ [s^{-1}]	10^{-3}
Reference stress	σ_0 [MPa]	201.1
Stress power index	n	5.622

Six cases of N (the number of randomly laminated fin layers) were considered, i.e. $N = 10$, 20, 40, 60, 80 and 100. For each case, 10 patterns of random misalignment were prepared using random numbers generated by a computer.

Substructures A_i were defined as illustrated in Fig. 3, and were divided into four-node isoparametric elements. The substructures were two-dimensional rather than three-dimensional, and the generalized plane strain condition was considered, because the plate-fin structures were assumed to have uniform and infinite material distribution in the y_3-direction.

A base metal for the plate-fin structures was Hastelloy X, which was a Ni-based alloy with excellent heat resistance. The Hastelloy X was regarded as an isotropic elastic-viscoplastic material characterized by the following constitutive equation [4]:

$$\dot{\varepsilon}_{ij} = \frac{1+\nu}{E}\dot{\sigma}_{ij} - \frac{\nu}{E}\dot{\sigma}_{kk}\delta_{ij} + \frac{3}{2}\dot{\varepsilon}_0\left(\frac{\sigma_{eq}}{\sigma_0}\right)^{n-1}\frac{s_{ij}}{\sigma_0}, \tag{26}$$

where, E and ν indicate elastic constants, $\dot{\varepsilon}_0$ and σ_0 represent reference strain rate and reference stress, respectively, n is a material parameter of viscoplasticity, s_{ij} stands for the deviatoric part of σ_{ij}, and $\sigma_{eq} = [(3/2)s_{ij}s_{ij}]^{1/2}$. Material constants used are listed in Table 1 [4].

Macroscopic uniaxial tension in the y_1-direction at a constant strain rate 10^{-3} [s^{-1}] was applied to the plate-fin structures.

4 Results of Analysis

First, Fig. 4(a) shows the macroscopic stress-strain relations of the plate-fin structures with random laminate misalignment subjected to uniaxial tension in the y_1-direction. However, only the results for $N = 100$ (solid lines) are shown in the figure due to limitations of space. In addition, the figure contains the results for $N = 1$ (dashed lines), i.e. the case of

no laminate misalignment ($d=0$) and the case of periodic laminate misalignment with half width of the substructure ($d=l/2$), where l indicates the width of the substructure. It can be seen from Fig. 4(a) that the viscoplastic flow stresses for the ultra-fine plate-fin structures with random laminate misalignment are situated between $d=0$ and $d=l/2$ for all the 10 patterns. This suggests that random plate-fin structures exhibit intermediate elastic-viscoplastic behavior between $d=0$ and $d=l/2$, and that the results for $d=0$ and $d=l/2$ can be the lower and upper bounds, respectively.

Next, Fig. 4(b) shows the relations between macroscopic strains in the y_1 -direction (loading direction), E_{11}, and in the y_2 -direction, E_{22}, i.e. macroscopic compressibility for the y_1 -direction loading. This figure contains the results for $N=100$ (solid lines) and $N=1$ (dashed lines). In addition, the dashed-dotted line indicates the isotropic incompressible case. As seen from the figure, macroscopic compressibility exhibits the same tendency as observed in the macroscopic stress-strain relations shown before, i.e. all the 10 patterns of random laminate misalignment result in the intermediate behavior between $d=0$ and $d=l/2$.

Finally, Figs. 5(a) and 5(b) respectively show the macroscopic stress Σ_{11} and the macroscopic strain E_{22} at $E_{11}=0.004$ when changing *N*. For $N=1$, the results for five cases of periodic laminate misalignment, i.e. $d=0$, $l/8$, $l/4$, $3l/8$ and $l/2$ are shown in the figures. It is seen from these figures that the dispersion of Σ_{11} and E_{22} decreases with the increase in *N*, and that they converge the intermediate values between $d=0$ and $d=l/2$.

5 Conclusions

In this study, elastic-viscoplastic properties and macroscopic compressibility of ultra-fine plate-fin structures with random laminate misalignment subjected to uniaxial tension were analyzed using a newly proposed method based on the time-dependent homogenization theory. In the proposed method, a unit cell of a plate-fin structure with randomly misaligned *N* fin layers is defined. The *Y*-periodic boundary condition is used on the side boundary surfaces of the unit cell, whereas the boundary condition for periodic laminate misalignment is applied on the top and bottom boundary surfaces. The unit cell is then divided into *N* substructures to introduce the substructure method into the time-dependet homogenization theory.

The analysis was performed for six cases of *N*, i.e. $N=10$, 20, 40, 60, 80 and 100, and macroscopic behavior of plate-fin structures was discussed. The analysis results showed that elastic-viscoplastic behavior of ultra-fine plate-fin structures with random laminate misalignment was intermediate between no misalignment case ($d=0$) and half a cell misalignment case ($d=l/2$). The results suggest that it is of importance to consider the laminate misalignment of ultra-fine plate-fin structures when analyzing their elastic-viscoplastic properties, and that the lower and upper bounds of the elastic-viscoplastic properties may be predictable from the results for $d=0$ and $d=l/2$.

References

[1] S. Ishiyama, and Y. Muto "High Temperature Mechanical Properties on Multi Stage Blazed Fin Body with Ultra Fine Off-Set Fin for Compact Heat Exchanger". *JSME Int. J, Ser. A*, Vol. 69, pp. 682-688, 2003.

[2] F. Kawashima, T. Igari, Y. Miyoshi, Y. Kamito and M. Tanihira "High temperature strength and inelastic behavior of plate-fin structures for HTGR". *Nucl. Eng. Des.*, Vol. 237, pp. 591-599, 2007.

[3] K. Kunitomi, S. Katanishi, S. Takada, T. Takizuka and X. Yan "Japan's future HTR-the GTHTR300". *Nucl. Eng. Des.*, Vol. 233, pp. 309-327, 2004.

[4] M. Tsuda, E. Takemura, T. Asada, N. Ohno and T. Igari "Homogenized elastic-viscoplastic behavior of plate-fin structures at high temperatures". *Int. J. Mech. Sci.*, Vol. 52, pp. 684-656, 2010.

[5] N. Ohno, X. Wu and T. Matsuda "Homogenized properties of elastic-viscoplastic composites with periodic internal structures". *Int. J. Mech. Sci.*, Vol. 42, pp. 1519-1536, 2000.

[6] O.C. Zienkiewicz and R.L. Taylor "The finite element method (5th edn.)". *Butterworth-Heinemann*, 2000.

[7] N. Yamamoto and T. Matsuda "Effects of laminate misalignment on elastic-viscoplastic properties of ultrafine plate-fin structures analysis using time dependent homogenisation theory". *Mater. Res. Innov.*, Vol. 15, pp. 147-150, 2011.

[8] T. Matsuda, S. Kanamaru, N. Yamamoto and Y. Fukuda "A homogenization theory for elastic-viscoplastic materials with misaligned internal structures". *Int. J. Plast.*, (in press).

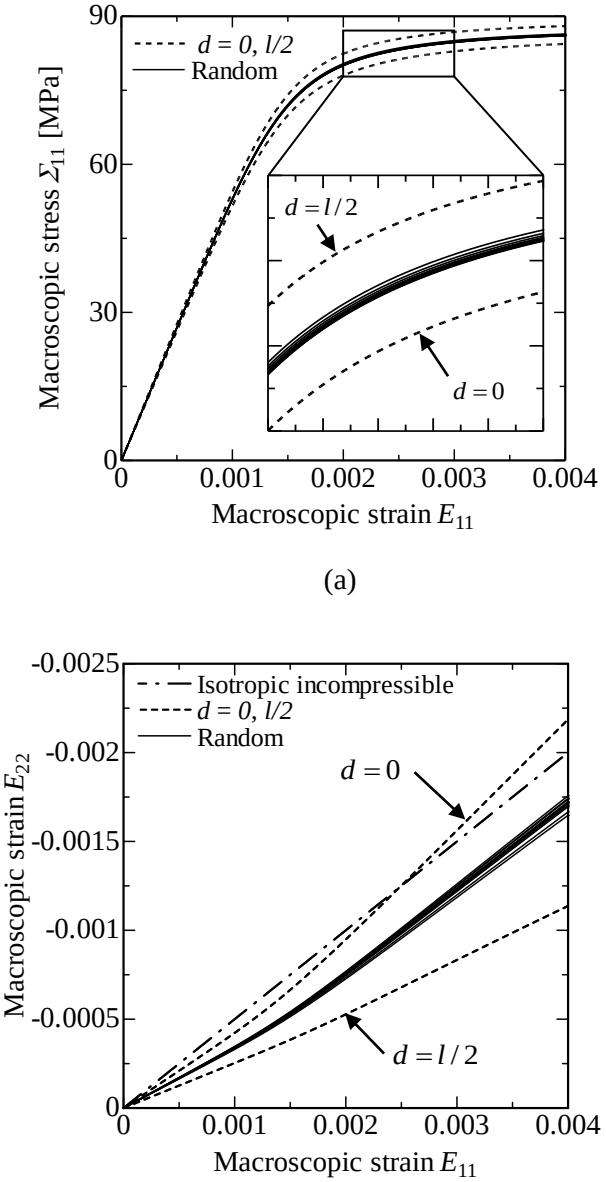

(a)

(a)

(b)

Fig. 4. Macroscopic behavior of ultra-fine plate-fin structures for ten cases of random laminate misalignment under uniaxial tension to the y_1-direction ($N = 100$); (a) stress-strain relations, (b) compressibility.

Fig. 5. Effects of the number of substructures N on macroscopic behavior of ultra-fine plate-fin structures under uniaxial tension to the y_1-direction; (a) Σ_{11}, (b) E_{22} ($E_{11} = 0.004$).